Int. J. Heat Mass Transfer. Vol. 10, pp. 1469–1484. Pergamon Press Ltd. 1967. Printed in Great Britain

THE MECHANISM OF NUCLEATE BOILING IN PURE LIQUIDS AND IN BINARY MIXTURES—PART III

S. J. D. VAN STRALEN†

Heat Transfer Section, Technological University, Eindhoven, The Netherlands

(*Received* 6 *February* 1967)

Abstract—Corrections on the author's "relaxation microlayer" theory of the mechanism of nucleate pool boiling have been made to account for the large peak flux occurring at a low concentration of the more volatile component in binary liquid mixtures, cf. Parts I–II. The removal of heat from the heating surface occurs during the greatest part of the adherence time and the entire subsequent delay time (i.e. almost continuously) and can be described by pure conduction only. Consequently, Gunther and Kreith's hypothesis of "microconvection in the normally laminar sublayer" is shown to be unnecessary. An expression for the peak flux has been derived in dependence on the corresponding convective contribution. In pure liquids, the direct vapour production at the wall is shown to be responsible for the entire increase in heat flux above convection at arbitrary superheating in the region of nucleate boiling, in quantitative agreement with experimental data, deduced from high-speed motion pictures on water.

Both the bubble departure radius and the peak flux are studied in dependence on pressure. The bubble size decreases rapidly at increasing pressure, in quantitative agreement with data on water by Séméria at elevated pressures and by the author at subatmospheric pressures. The critical superheating in nucleate boiling is shown to diminish at increasing pressure, in agreement with Addoms' data.

The favourable effect of a slight degree of fouling at the heating surface on the nucleation properties and consequently on the corresponding coefficient of heat transfer, which had been discovered previously by the author, is discussed in comparison with more recent additional results by other workers. Finally, the occurrence of a hysteresis effect in boiling is shown to be due to fouling.

ADDITIONAL NOMENCLATURE‡

d^*, $= d\,\theta_0/(\theta_0 + \theta_0^*)$, instantaneous thickness of superheated part of relaxation microlayer in surface boiling [μ or m];

f, $= 2100$ for water at arbitrary pressure, $f = 460$ for ethanol [J/m$^{\frac{1}{2}}$s$^{\frac{1}{2}}$(degC)$^{\frac{1}{2}}$];

L^*, distance to heating wire of collapsing vapour bubble in surface boiling [m];

p, absolute pressure [ata], 1 ata = $0{\cdot}981 \times 10^5$ N/m^2;

$p_{1,\infty}$, partial vapour pressure of water at a plane surface of liquid containing a mole fraction x_M of the more volatile component (ethanol) [N/m^2];

p_{1,R_0^*}, partial vapour pressure of water at a convex liquid surface (with radius of curvature R_0^*) containing a mole fraction x_M of ethanol [N/m^2];

$p_{2,\infty}$, partial vapour pressure of ethanol at a plane surface of water–ethanol liquid mixture containing a mole fraction x_M of ethanol [N/m^2];

p_{2,R_0^*}, partial vapour pressure of ethanol at a convex liquid surface (with radius of curvature R_0^*) containing a mole fraction x_M of ethanol [N/m^2];

R^*, instantaneous radius of equivalent spherical bubble during condensation in surface boiling [m];

R_1^*, maximum radius of equivalent spherical bubble in surface boiling [m];

† Doctor of Physics, Principal Research Officer.

‡ See Nomenclature in Part I [2].

R_0^*, radius of equilibrium nucleus for dropwise condensation [m];
R_g, $= 8{\cdot}314 \times 10^3$, universal gas constant [J/°K kmol];
S, dimensionless critical (minimal) supersaturation for condensation of vapour;
t_1^*, instant at which maximum bubble radius in surface boiling is reached [s];
t_3^*, condensation time of bubble in surface boiling [s];
$t_1^* + t_3^*$, time between collapse and initial formation of bubble, or lifetime of bubble in surface boiling [s];
T_0, absolute temperature of bulk liquid in surface boiling, or absolute temperature of vapour mixture in cloud chamber [°K];
v', propagation velocity of ultrasonic waves in liquids [m/s];
V', molar volume of mixture in liquid drop [m^3/kmol];
V_∞, characteristic liquid flow velocity at relatively great distance to heating surface [m/s].

Greek symbols

α', absorption coefficient of liquid for ultrasonic waves [1/m];
α'', $= \alpha'/(\nu')^2$, modified frequency-independent absorption coefficient of liquid for ultrasonic waves [s^2/m];
η, (liquid) dynamic viscosity ($2{\cdot}8 \times 10^{-4}$ for water at atmospheric boiling point [kg/sm]);
θ_0^*, $= T - T_0$, difference between saturation temperature and temperature of bulk liquid in surface boiling, or (degree of) subcooling [degC];
ν', frequency of ultrasonic waves [1/s];
ζ, dimensionless integration variable.

Superscripts

(•), value for ethanol;
(*), value for surface boiling of subcooled liquid.

1. INTRODUCTION

ACCORDING to a private communication by Professor Forster, Forster and Greif [1] suggested a "vapour–liquid exchange action" previously, which is in certain respects similar to the author's "relaxation microlayer" theory [2, 3] for nucleate boiling. Both mechanisms are fundamentally based on a periodic removal of the superheated thermal boundary layer away from the heating surface, which is due to the rapid initial growth of succeeding vapour bubbles on active nuclei. However, there remain essential distinctions between the two conceptions. The effect of initial bubble growth rates and frequencies is insufficiently incorporated in the resulting correlations of Forster and Greif.

The author's theory is extended here to a simple relation for the peak flux, which is suitable for application to cases of practical interest. Heat conduction is shown to result in sufficiently large heat flux values to account for the observed large peak fluxes in binary mixtures at a certain (low) concentration of the more volatile component. Gunther and Kreith's [4] hypothesis of "some form of random microconvection excited by bubble activity in the normally laminar sublayer", which is discussed extensively in [1], is thus unnecessary. A comparison of conduction is made with Pohlhausen's equation, cf. [5] for forced laminar flow.

Some aspects of fouling of the heating surface during pool boiling are discussed.

The shorter duration of the sudden temperature dips occurring at the heating surface [6, 7] in coincidence with initial bubble growth [8, 9], compared to the adherence time is explained. The theoretical bubble departure radius in water, boiling at pressures from 0·10 to 100 ata, is compared with data by Van Stralen [10] for low pressures and by Séméria [11] for elevated pressures.

Additional investigations have been carried

out for bubbles in nucleate boiling and film boiling of ethanol at atmospheric pressure. An expression is derived for the maximum bubble radius in dependence on the degree of subcooling, cf. Part IV.

2. THE NUCLEATE BOILING PEAK FLUX ACCORDING TO THE EXTENDED RELAXATION MICROLAYER THEORY

Objections may be raised to the derivation of equations (11, 12, 72) of Part II [3] in case of binary mixtures, because the required increase in heat flux (in the ratio $C_{1,p}/C_{1,m}$) during the decreased delay time t_2 cannot be accounted for by pure conduction only. This deficiency can be removed by restricting the validity of these equations to the area of a small central circle in the region of influence A_i (cf. equation (19) of [3]) of a bubble in the thermal boundary layer at the heating surface. The superheating of the remaining major part of A_i occurs not only during the delay time, but starts already during the time of adherence (i.e. one can say with some exaggeration, that heating occurs during any complete bubble cycle, thus continuously). The reader is referred to Fig. 4 of Part I [2], where a contraction of the vapour–solid contact area at the base of a bubble before departure is shown.

The correction is of minor importance in pure liquids, as it follows from equation (9) of [3], that:

$$t_2 = 3\left(\frac{C_{1,m}}{C_{1,p}}\right)^2 t_1, \tag{1}$$

whence $t_1 + t_2 = (\frac{4}{3})t_2$ for pure liquids; $t_1 + t_2 \gg t_2$ for mixtures with a relatively small $C_{1,m}$, which results in a considerably prolonged heating time.

The proposed improvement of the theory is also in accordance with the relatively short duration of the temperature dips, which were shown to respond to the local liquid temperature at some distance of a bubble centre. The incorrect interpretations of these fluctuations by Moore and Mesler [6] and Bonnet, Macke and Morin [9], cf. Section 1.4 of Part I [2], are denied directly by recent experiments of Macke [12]. This worker observed temperature fluctuations up to 3 degC in the liquid at short distances above the heating surface.

Apparently, the theory remains valid to predict the behaviour of the local superheating very close to an active nucleus and consequently also for derivative quantities, e.g. the bubble frequency. For the derivation of the heat flux at the heating surface, however, one has to replace t_2 by $t_1 + t_2$, whence equation for $\bar{q}_{w,i}$ in Section 1 of [3] has to be changed into:

$$q_{w,bi,\max} = \frac{2}{\pi^{\frac{1}{2}}}(k\rho_1 c)^{\frac{1}{2}} v_{\max}^{\frac{1}{2}} \theta_{0,\max}\left(1 - \frac{1}{e}\right). \tag{2}$$

Contrarily, equation (65) of [3] remains unaltered:

$$q_{w,b,\max} = \rho_2 l C_1 t_{1,\max}^{\frac{1}{2}} v_{\max} \theta_{0,\max}\left(1 - \frac{1}{e}\right). \tag{3}$$

2.1. *Pure liquids*

It follows from equation (1): $t_2 = 3t_1$, thus $v = 1/(4t_1)$, whence equation (3) yields at peak flux conditions:

$$q_{w,b,p,\max} = \frac{1}{2}\left(\frac{3}{\pi}\right)^{\frac{1}{2}}(k\rho_1 c)^{\frac{1}{2}} \frac{1}{t_{1,p,\max}^{\frac{1}{2}}} \times \theta_{0,p,\max}\left(1 - \frac{1}{e}\right). \tag{4}$$

It follows from equations (2), that:

$$q_{w,bi,p,\max} = \frac{1}{\pi^{\frac{1}{2}}}(k\rho_1 c)^{\frac{1}{2}} \frac{1}{t_{1,p,\max}^{\frac{1}{2}}} \times \theta_{0,p,\max}\left(1 - \frac{1}{e}\right). \tag{5}$$

Equation (5) is predicting a 1·15 times increased value in comparison to equation (4). By taking the duration of the temperature dips {i.e. $(15/100)\ 4t_1 \approx 3 \times 10^{-3}$ s, in good agreement with [7] and [8]} into account, it is seen, that:

$$q_{w,b,p,\max} = q_{w,bi,p,\max}, \tag{6}$$

i.e. equation (70) of [3] again. The validity of

this equation can be extended to the entire region of nucleate boiling:

$$q_{w,b,p} = q_{w,bi,p}. \tag{7}$$

Consequently,

$$q_{w,p} = q_{w,bi,p} + q_{w,co,p} = q_{w,b,p} + q_{w,co,p}. \tag{8}$$

This theoretical expression is in quantitative agreement with experiments on water, boiling at atmospheric pressure (Fig. 1). These results are deduced from high-speed motion pictures (6000 frames per s) by measuring the direct vapour formation at the heating wire. The corresponding $q_{w,b,p}$ is compared with the entire increase $q_{w,bi,p}$ of $q_{w,p}$ above the convective contribution, which has been extrapolated to the region of nucleate boiling, cf. also Table 1 of [2]. The agreement justifies the theoretical mechanism.

2.2. *Binary mixtures*

$C_{1,m} = 0{\cdot}25\ C_{1,p}$ is taken, which occurs in 4·1 wt. % methylethylketone in water, cf. Section 2.4 of [3] and Table 2 of [3]. In this case it follows from equation (8) of [3], that $t_{2,m} = 3(C_{1,m}/C_{1,p})^2\ t_{1,m} = (\frac{3}{16})\ t_{1,m}$. Equation (3) yields now:

$$q_{w,b,m,\max} = \frac{8}{19}\left(\frac{3}{\pi}\right)^{\frac{1}{2}} (k\rho_1 c)^{\frac{1}{2}} \frac{1}{t_{1,m,\max}^{\frac{1}{2}}} \times \theta_{0,m,\max}\left(1 - \frac{1}{e}\right) \tag{9}$$

and equation (2) is giving

$$q_{w,bi,m,\max} = \frac{8}{(19\pi)^{\frac{1}{2}}} (k\rho_1 c)^{\frac{1}{2}} \frac{1}{t_{1,m,\max}^{\frac{1}{2}}} \times \theta_{0,m,\max}\left(1 - \frac{1}{e}\right). \tag{10}$$

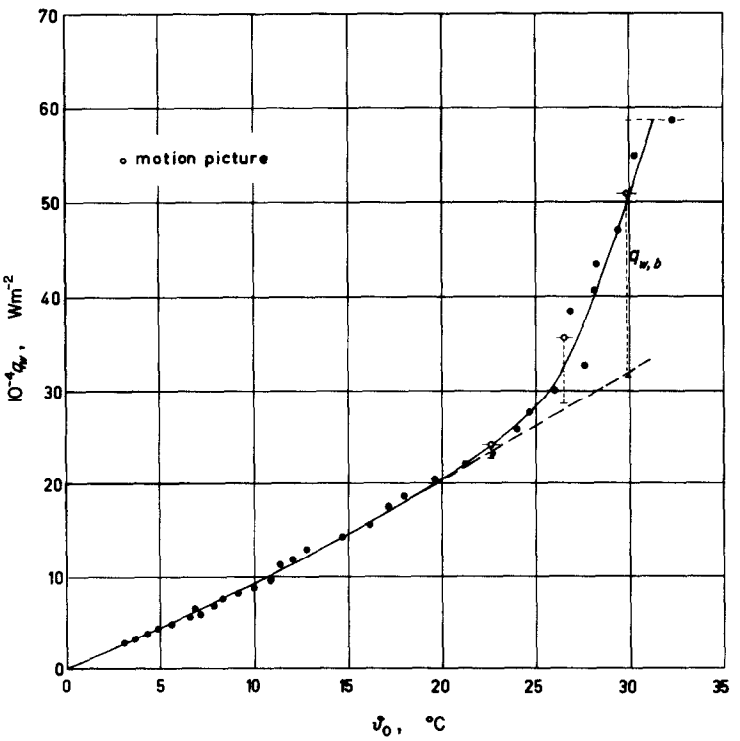

FIG. 1. *Water.* Boiling curve at atmospheric pressure. The experimental contribution $q_{w,b}$ of the direct vapour formation at the heating surface (which has been deduced from simultaneous high speed motion pictures), equals the entire increase $q_{w,bi}$ in heat flux density above the convective contribution.

One has thus for this mixture:

$$q_{w,bi,m,\max} = (\tfrac{19}{3})^{\frac{1}{4}}\, q_{w,b,m,\max} = 2{\cdot}52\, q_{w,b,m,\max}. \tag{11}$$

The critical wire temperature in nucleate boiling is (for small additions) independent of the composition of the mixture [13], whence:

$$\theta_{0,m,\max} = \theta_{0,p,\max} + (T_p - T_m). \tag{12}$$

The average departure time $\bar{t}_1$ (and consequently also t_2 and v) is determined both in mixtures and in pure liquids by the excess enthalpy balance, i.e. the condition (28) of [3], whence:

$$d_{0,p} = \frac{\rho_2 l}{\rho_1 c} C_{1,p} \bar{t}_1^{\frac{1}{2}} = \left(\frac{12}{\pi} a \bar{t}_1\right)^{\frac{1}{2}} = \frac{\mathrm{e}}{2(\mathrm{e}-1)} \frac{k}{h_{w,co}}. \tag{13}$$

It is seen from equations (8, 5, 13), that in general for pure liquids:

$$q_{w,p,\max} = \left[\frac{4}{\pi}\sqrt{3}\left(1 - \frac{1}{\mathrm{e}}\right)^2 + 1\right] q_{w,co,p,\max} = 1{\cdot}88\, q_{w,co,p,\max}. \tag{14}$$

The decreased peak flux in organic liquids in comparison to water is thus due to a corresponding lower convective heat transfer, which is partly annulled by an increased $\theta_{0,\max}$, cf. Fig. 1 of [2].

It follows from equation (10), that for the mixture under consideration:

$$q_{w,m,\max} = 2{\cdot}62\, q_{w,co,m,\max}. \tag{15}$$

For free convection from horizontal heating cylinders $q_{w,co,\max} \sim \theta_{0,\max}^{1{\cdot}25}$ in a large laminar range of $(Gr \,.\, Pr)$-values, whence (cf. Table 3 of [3]) one has for 4·1% methylethylketone in comparison to water:

$$q_{w,m,\max} = 2{\cdot}47\, q_{w,p,\max}. \tag{16}$$

The values of this ratio is in quantitative agreement with experimental data for a combination of natural and forced convection, cf. Section 1.2 of [2].

Formally, the action of the bubbles can be considered as an increase of the convection. The peak flux may thus be expressed in extended correlations for convective heat transfer.

The following expression, deduced by making use of (1), is valid more generally than (15) for arbitrary values of $C_{1,m}$:

$$q_{w,m,\max} = \left\{\frac{(8/\pi)(\sqrt{3})(1 - 1/\mathrm{e})^2}{[1 + 3(C_{1,m}/C_{1,p})^2]^{\frac{1}{2}}} + 1\right\} \times q_{w,co,m,\max}. \tag{17}$$

Equation (17) yields in combination with (14) in case of $C_{1,m} \ll C_{1,p}$, which applies, e.g. (i) to mixtures in pool boiling, (ii) to pure liquids boiling at elevated pressures, and (iii) to surface boiling (Part IV):

$$q_{w,m,\max} = (2q_{w,p,\max} - q_{w,co,p,\max}) \times \frac{q_{w,co,m,\max}}{q_{w,co,p,\max}}. \tag{18}$$

The subscripts m and p refer here for (i) and (iii): to the peak flux in the mixture and in the less volatile pure component, and for (ii): to the peak flux at the ambient pressure and at atmospheric pressure, respectively. It is seen from equations (18) and (12), that an upper boundary both for nucleate and surface boiling on horizontal cylinders is given by:

$$q_{w,m,\max} = 1{\cdot}47\, q_{w,p,\max}\left(1 + \frac{T_p - T_m}{\theta_{0,p,\max}}\right)^{1{\cdot}25}. \tag{19}$$

The treatment in the case of cylinders and plates in the turbulent range, in which the value of the exponent has been increased to 1·33, is analogous.

The reader is referred to the Appendix for a comparison with experimental data.

2.3. *Comparison with Pohlhausen's equation*

Pohlhausen's solution for forced laminar flow parallel to a plane heating plate [5, 14] can also be used for the derivation of $q_{w,bi,\max}$. The characteristic velocity V_∞ at great distance to the plate and the characteristic distance on the plate have to be adjusted properly to the special

problem under consideration. A cylindrical microlayer volume $A_i d_0$ has to be superheated here, whence the velocity is following from: $2\pi R_i(\frac{1}{2}V_\infty)\, d_0(t_1 + t_2) = A_i d_0 = \pi R_i^2 d_0$, or $V_\infty = vR_i$. The characteristic distance equals the radius $R_i = (A_i/\pi)^{\frac{1}{2}}$ of the region of influence.

The resulting expression for the heat flux turns out to be independent of R_i:

$$q_{w,bi,\max} = 2 \times 0{\cdot}806\, k \left(\frac{\rho_1 V_\infty}{\eta R_i}\right)^{\frac{1}{2}} \theta_{0,\max} \left(1 - \frac{1}{e}\right)$$
$$= 1{\cdot}612\, k \left(\frac{\rho_1}{\eta}\right)^{\frac{1}{2}} v^{\frac{1}{2}}\, \theta_{0,\max} \left(1 - \frac{1}{e}\right). \qquad (20)$$

The factor 2 originates from taking the average value during the heating time, cf. the equation for $\bar{q}_{w,i}$ in Section 1 of [3], and the numerical factor 0·806 from the value of $Pr = \eta/\rho_1 a$ for water at 100 degC.

Satisfactorily, equation (20) yields nearly 10 per cent higher values in comparison with (2) for pure conduction. Both equations agree in predicting $q_{w,bi,\max} \sim v^{\frac{1}{2}}\theta_{0,\max}$. The increase in the nucleate boiling peak flux is thus shown explicitly to depend on a higher bubble frequency, i.e. the frequency of the periodic removal of a quantity of hot liquid away from the wall.

3. THE PEAK FLUX AND THE CRITICAL SUPERHEATING AT ELEVATED PRESSURES

Van Stralen [15, 16] deduced an empirical relation from the boiling curves on horizontal 500 μ platinum wires by Addoms [17, 18] for water (200 μ wires are already representative for large heating surfaces):

$$h_{w,p,\max} C_{1,p}^{\frac{1}{2}} = 2100\ \mathrm{J\,m^{-\frac{1}{2}}\,s^{-\frac{1}{2}}\,(degC)^{-\frac{1}{2}}}. \qquad (21)$$

The numerical value of the constant in the right-hand side is independent of pressure, up to the critical pressure. Equation (21) explains the increase of the peak flux (which is proportional to $\rho_2^{\frac{1}{2}} \sim p^{\frac{1}{2}}$) up to a third of the critical pressure.

From equations (21, 5, 14) it follows:

$$v_{p,\max}^{\frac{1}{2}} = \frac{\pi^{\frac{1}{2}}}{2}\frac{88}{188}\frac{e}{e-1}\frac{2100}{(k\rho_1 c C_{1,p})^{\frac{1}{2}}}, \qquad (22)$$

whence the bubble frequency increases linearly with $\rho_2 \sim p$. Equation (22) predicts for water, boiling at atmospheric pressure, a maximal frequency of approximately 150 s^{-1}, which is in good agreement with $t_{1,p,\max}^{\frac{1}{2}} = 4{\cdot}09 \times 10^{-2}\ \mathrm{s^{\frac{1}{2}}}$; cf. the Appendix.

A generalized equation for binary mixtures with water in excess following from (21) is proposed:

$$h_{w,m,\max} C_{1,m}^{\frac{1}{2}} = h_{w,p,\max} C_{1,p}^{\frac{1}{2}}$$
$$= 2100\ \mathrm{J\,m^{-\frac{1}{2}}\,s^{-\frac{1}{2}}\,(degC)^{-\frac{1}{2}}}. \qquad (23)$$

The theoretical ratio $q_{w,m,\max}/q_{w,p,\max}$ for the maximum value obtained by adding methylethylketone to water amounts thus to 2·0, a value which is in good agreement with the experimental data in the range from 10 to 50 ata, Fig. 2 and [13]. Quantitative agreement is also obtained at atmospheric pressure for 4·1 % methylethylketone in comparison to water, where the experimental value of $h_{w,m,\max}/h_{w,p,\max} = 1{\cdot}75$ [13].

Zuber [19] and Zuber and Tribus [20] (cf. also Section 4.6 of [3]) derived an expression for the peak flux in nucleate pool boiling of pure liquids, which is in good agreement (Fig. 3) with experimental results up to the critical pressure for water by Kazakova [21] and for ethanol by Cichelli and Bonilla [22]:

$$q_{w,\max} = \frac{\pi}{24}\rho_2^{\frac{1}{2}}\, l\{\sigma g(\rho_1 - \rho_2)\}^{\frac{1}{2}}. \qquad (24)$$

This equation predicts a relatively high peak flux for water at atmospheric pressure, viz. $111 \times 10^4\ \mathrm{W/m^2}$. Equation (24) is not valid for binary mixtures, as e.g. a lower peak flux is predicted (on account of a decreased surface tension) for 4·1 % methylethylketone in comparison to water, instead of a considerably increased peak flux.

According to (24), $q_{w,\max} = 0$ at the critical

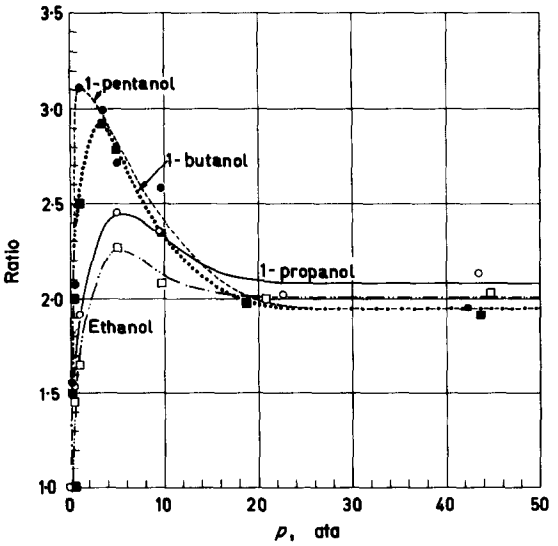

FIG. 2. *Water–ethanol, water–1-propanol, water–1-butanol and water–1-pentanol.* Ratio of maximum peak flux in binary mixtures to corresponding value in water in dependence on pressure.

Maximal ratios between 2·3 and 3·1 occur at relatively low pressures between 1 and 10 ata. The ratios approximate the value 2·0 in the range from 20 to 50 ata.

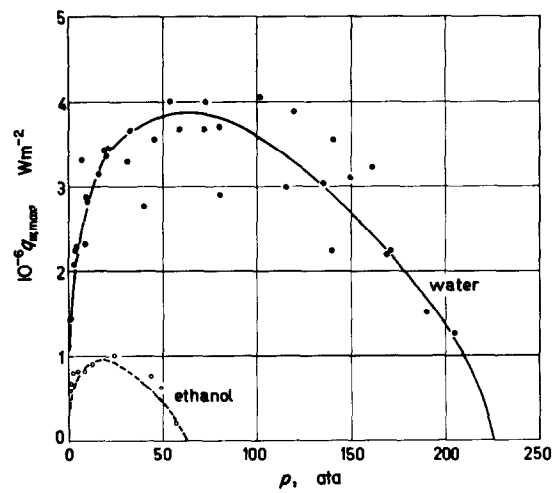

FIG. 3. *Water and ethanol.* Peak flux density in dependence on pressure. The theoretical Zuber–Tribus curves are compared with experimental data by Kazakova for water and by Cichelli and Bonilla for ethanol.

conditions; actually, of course $q_{w,\max} > 0$ then, whence the development of supercritical heterogeneous water and natrium nuclear reactors is made possible.

Combination of (24) with (21) is yielding an expression for the maximal superheating in nucleate boiling:

$$\theta_{0,\max} = \frac{\pi}{24}\frac{1}{2100}\left(\frac{12}{\pi}\right)^{\frac{1}{4}} l^{\frac{1}{4}}\{\sigma g(\rho_1 - \rho_2)k\rho_1 c\}^{\frac{1}{4}}, \tag{25}$$

whence $\theta_{0,\max} \to 0$ at the critical pressure, in agreement with Addoms' results [17, 18]. Equation (25) predicts a $\theta_{0,\max} = 40{\cdot}6$ degC at atmospheric pressure, which is 1·5–2·0 times too high.

It may be worth noticing, that the numerical constant (2100) in equations (21, 22, 23, 25) is not universal, since a lower value must occur in ethanol. In principle, the value of this constant might be evaluated by making use of equation (14), provided that the equivalent conduction layer, which corresponds with the convective contribution, should be renewed completely in each bubble cycle. It is quite a question whether this statement holds at high pressures, as the frequent occurrence of bubble coalescences may have a serious effect on the relaxation microlayer thickness.

Kwanten [23] has shown, that equation (25), but with a six times larger numerical value of the constant, viz. $5{\cdot}5 \times 10^{-4}$ J^{-1} m$^{\frac{1}{4}}$ s$^{\frac{1}{4}}$ (degC)$^{\frac{1}{4}}$ instead of $(\pi/24)(1/2100)(12/\pi)^{\frac{1}{4}}$, is in reasonable agreement with experimental data for a large number of pure liquids, boiling at atmospheric pressure. The data include e.g. values for liquid H_2, O_2, N_2, He, methanol, carbontetrachloride, 1-butanol, toluene, benzene and pentane. The corresponding $\theta_{0,\max}$ varies from 1·7 degC (for H_2) to 55 degC (for methanol). Hence, the validity of equation (21) is thus extended to pure organic liquids by reducing the constant in the right-hand side to 350 J m$^{-\frac{1}{4}}$ s$^{-\frac{1}{4}}$ (degC)$^{-\frac{1}{4}}$; the agreement includes then also data for ethanol (Fig. 3) and for methylethylketone (Fig. 1 of [2]).

The numerical value of the constant f [$= 2100$ J m$^{-\frac{1}{2}}$ s$^{-\frac{1}{2}}$ (degC)$^{-\frac{1}{2}}$ for water] in the right-hand side of equation (21) can be estimated easily for organic liquids, e.g. for ethanol in comparison to water. The quantities for ethanol are denoted with a (•). Combination of (21) and (14) is giving:

$$\frac{2100}{f} = \left(\frac{q_{w,p,\max}}{\theta_{0,\max}} \Big/ \frac{q^{\bullet}_{w,p,\max}}{\theta^{\bullet}_{0,\max}}\right)\left(\frac{C_{1,p}}{C^{\bullet}_{1,p}}\right)^{\frac{1}{2}} \approx \left(\frac{k}{k^{\bullet}}\right)^{\frac{1}{2}}\left(\frac{C_{1,p}}{C^{\bullet}_{1,p}}\right)^{\frac{1}{2}} \simeq (4)^{\frac{1}{2}}\left(\frac{24}{9}\right)^{\frac{1}{2}} = 4{\cdot}6, \quad (26)$$

whence $f = 460$ J m$^{-\frac{1}{2}}$ s$^{-\frac{1}{2}}$ (degC)$^{-\frac{1}{2}}$. This approximation may be used, as the lower convective contribution in ethanol is mainly due to a four times smaller thermal conductivity at the atmospheric boiling point. The factor 4·6 in the right-hand side of (26) agrees reasonably with Kwanten's factor 6, and also with the maximum peak fluxes occurring in both liquids (Fig. 3).

The most general semi-empirical expressions for the maximum heat transfer and the corresponding critical superheating both in pure liquids and binary mixtures (containing the main component in excess) are thus the following generalizations of equations (21) and (25), respectively (in SI-units):

$$h_{w,\max} C_1^{\frac{1}{2}} = 2800\, k^{\frac{1}{2}} \quad (27)$$

and

$$\theta_{0,\max} = \frac{\pi}{24}\frac{1}{2800}\left(\frac{12}{\pi}\right)^{\frac{1}{2}}\left(\frac{l}{k}\right)^{\frac{1}{2}} \times \{\sigma g(\rho_1 - \rho_2)\rho_1 c\}^{\frac{1}{2}}. \quad (28)$$

In the derivation of these equations, use has been made of (26), and the thermal conductivity has been assumed to be independent of pressure. In principle, any boiling curve is determined by these equations. Actually, however, deviations up to a factor 2, occur in the experimental data for the same liquid on various heating wires. The behaviour of very thin heating wires is included in the predictions of (28), as $\theta_{0,\max}$ is independent of the diameter, but not yet in those of (27) as $q_{w,co} \sim$ (diameter)$^{-\frac{1}{2}}$; the peak flux on a 3-μ wire in water, boiling at atmospheric pressure, has actually been increased to approximately 300×10^4 W/m^2 [15, 16]. Apparently, equation (27) can easily be extended to this case, which is, of course, of minor importance for practical utilizations.

4. THE PEAK FLUX IN ORGANIC LIQUIDS AND MIXTURES

The increase of the peak flux in organic mixtures in comparison to the values in the pure components, is in most cases restricted to 35 per cent, even in cases where a much higher increase should be expected on account of large numerical values of $\Delta T/G_d$ [13, 16, 23, 24, 25]. Apparently, this limitation is caused by a relatively low thermal diffusivity, whence the effect of $\Delta T/G_d$ in the denominator of the right-hand side of equation (12) of [2] is weakened by the factor $(a/D)^{\frac{1}{2}}$ in comparison with aqueous mixtures.

A low thermal diffusivity is also responsible for a low growth constant in pure organic liquids, e.g. for a theoretical and experimental [26] $C_{1,p} = 9 \times 10^{-4}$ m/s$^{\frac{1}{2}}$ degC in ethanol. This low growth constant coincides here with a low peak flux (40×10^4 W/m^2); this behaviour contrasts with that of binary mixtures with a more volatile component, but agrees with a low convective heat transfer, cf. equation (14); cf. also the similar boiling curve for 1-butanol in Fig. 1 of [2].

5. EFFECT OF THE SURFACE TENSION ON THE PEAK FLUX

A diminished tendency for coalescence of vapour bubbles in "positive" mixtures (i.e. the more volatile component has the lower surface tension constant) is predicted due to the Marangoni-effect, according to Hovestreijdt [24], cf. [3]. This is due to an exhaustion of the more volatile component in the liquid film between two neighbouring bubbles, which is causing a locally increased surface tension at the near-by parts of the bubble boundaries.

These interfaces are contracting and the bubbles are withdrawn from coalescence. Very densely populated bubble clusters can occur in these mixtures, cf. Figs. 3–4 of [2]. Only scarcely is coalescence observed here (Fig. 4). Apparently, bubble coalescence is always associated with oscillations about the spherical shape (Figs. 4 and 5).

Van Stralen [16] has shown, that the importance of the Marangoni-effect is most pronounced in case of a vertical heating wire. The peak flux in 4·1% methylethylketone and in 1·5% 1-butanol is practically independent of the orientation of the wire from horizontal to vertical.

Contrarily, the peak flux in water decreased from 59×10^4 W/m^2 on horizontal platinum wires to 45×10^4 W/m^2 on vertical wires at a constant $q_{w,co,\max} = 29 \times 10^4$ W/m^2. The corresponding maximal density of active nuclei decreased from 57×10^4 m^{-2} to 29×10^4 m^{-2}. Hence $q_{w,bi,\max} = 30 \times 10^4$ W/m^2 and 16×10^4 W/m^2, respectively, i.e. $q_{w,bi,\max} = q_{w,b,\max} \sim m_{\max}/A_w$, in accordance with equation (65) of [3]. The lower $m_{\max}/A_w$ on vertical wires is due to a coalescence of ascending bubbles from neighbouring nuclei, which causes a premature onset of film boiling at the upper part of the wire. The effect occurs also in narrow vertical tubes and channels. Apparently, the use of binary mixtures is most favourable in these geometrical designs.

A direct influence of the surface tension on the peak flux can hardly be observed; this is following from experiments by Van Stralen [27] on the addition of 1 vol. % of a foaming agent (Teepol) to water, boiling at a pressure of 0·13 ata. An intensive unstable foaming occurs at the liquid-level surface, but a slowing down of the bubble growth was also absent. The superheating, necessary to activate the first nucleus, has been decreased, since $R_0 = 2\sigma T/\rho_2 l\theta_0$ (Figs. 6 and 7).

6. FOULING OF THE HEATING SURFACE

In contradistinction to the negative result of the above mentioned experiment, the addition of Teepol to boiling water was more successful at atmospheric pressure [27]: the peak flux had been increased with a factor 2·5 by use of d.c. heating at a 1·7 times higher $\theta_{0,\max}$. When the experiment was completed, both the heating surface and the liquid had attained a yellowish colour, due to a thermal decomposition of the foaming agent. The increase and the contamination of the wire did not occur, when a peak flux equal to that for water, boiling at the same pressure, was determined rapidly for this solution with a.c. heating.

A contaminated wire showed also a 2·5 times increased peak flux in pure water. Obviously, the increased peak flux was caused only by the fouling of the heating surface and not by the foaming properties of the liquid, (Fig. 6).

A similar effect occurred at 0·13 ata in samples of skimmilk and whey diluted with water, due to a deposition of coagula on the wire.

Only a thin coagulation layer (< 20 μ) has a favourable effect on the peak flux, as a thicker layer, which is deposited rapidly in skimmilk boiling at atmospheric pressure, acted fairly well as an insulator. The increased peak flux and corresponding maximum $h_{w,\max}$ at low pressures are due to an increasing number of active nuclei (Figs. 6 and 7). The negative slope of a part of the boiling curve is due to the similar behaviour of the nucleation function [28], cf. also Fig. 8.

Farber and Scorah [29] investigated the effect of "farberizing" a nickel–chromium–iron alloy (Chromel-C) wire, i.e. of oxidation in film boiling under water at 1250°C. Both $q_{w,\max}$ and $\theta_{0,\max}$ could be increased a factor 2.

Ogden and Scorah [30] attributed this effect to the formation of a thin, hard film of chromium oxide with special properties on the surface.

Hampson, Turton and Sutherland [31] investigated the effect of the addition of fine powdered graphite (of 2–50 μ particle size), precipitated silica (2–50 μ) and emery powder (12–60 μ) to water as examples of insoluble

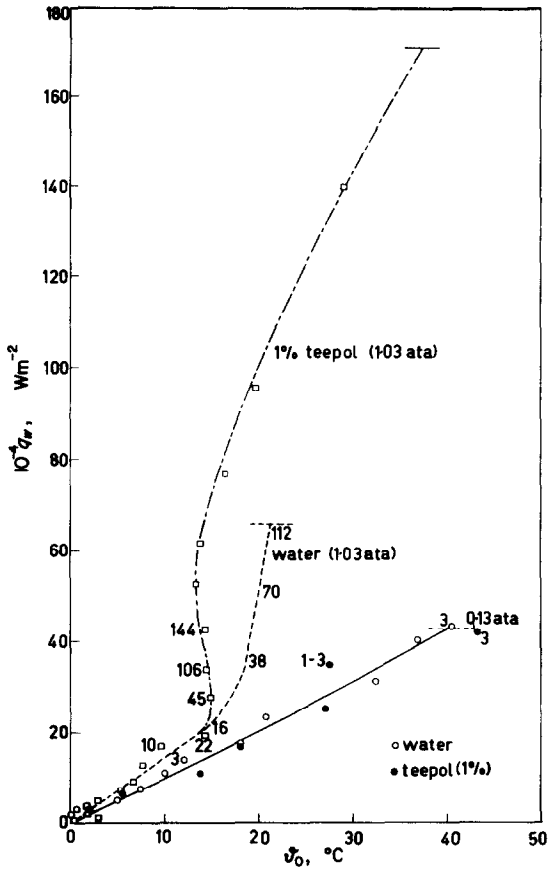

FIG. 6. Boiling curve for water and for a solution containing 1 vol. % of a dilute foaming agent (Teepol) in water, at atmospheric pressure and at a pressure of 0·13 ata. The figures at the curves denote the number of active nuclei generating vapour bubbles on a square cm of the platinum heating wire.

solids. In the first two cases a film was formed on the horizontal stainless steel heating tube during boiling. Similarly to the above-mentioned results [27], considerable increases (up to a factor 2) in the peak flux occurred, which were shown to be due to the fouling of the tube. Contrarily, the emery powder particles did not adhere to the tube, and the effect on the boiling curve was negligible.

Palen and Westwater [32] boiled aqueous solutions of calcium sulphate on electrically heated strips of oxidized aluminium. The "fouling curve" (θ_0 vs. time at constant q_w) shows for $q_w = 18 \times 10^4$ W/m^2 a maximum of 25 degC at 3 min and a minimum at 20 min, and increases then gradually. The deposition rate on the strip was nearly constant at constant q_w and proportional to q_w^2. The fouling activated additional nuclei, causing h_w to increase during a part of the boiling time, in agreement with the above mentioned results [27]. A thin coating of polyfluorohydrocarbon on the strip reduced the fouling during calcium sulphate deposition. These results are not generally valid, as the behaviour toluene–styrene was radically different.

A qualitative explanation of some of these phenomena with the relaxation microlayer theory seems to be possible. In Van Stralen's experiments [27], the bubble radius had been reduced considerably in comparison to water, whence an increased $q_{w,\max}$ is mainly due to a larger $m_{\max}/A_w$ and to a higher bubble frequency. In case of powdered graphite [31], the number of active nuclei decreased at constant q_w and constant bubble size, whence both $\theta_{0,\max}$ and $q_{w,\max}$ increase. In the experiments on calcium sulphate [32], the instantaneous increase in m/A_w causes a larger h_w.

7. HYSTERESIS EFFECT IN NUCLEATE BOILING

This effect is apparently due to a gradual fouling of the heating surface during nucleate boiling at increasing heat flux [13]. A consecutive gradual decrease of q_w results in a shift of the boiling curve to lower superheatings (Fig. 9), which is caused by the action of a relatively large number of nuclei generating generating vapour bubbles.

The behaviour in boiling during a long time is similarly [14]: the surface and the liquid are degassed gradually, causing a decrease in the number of active nuclei. The boiling curve is then shifted towards larger superheatings.

8. DEPENDENCE OF THE DEPARTURE RADIUS IN WATER BOILING AT SUBATMOSPHERIC AND ELEVATED PRESSURES

The growth constant C_1 decreases rapidly at

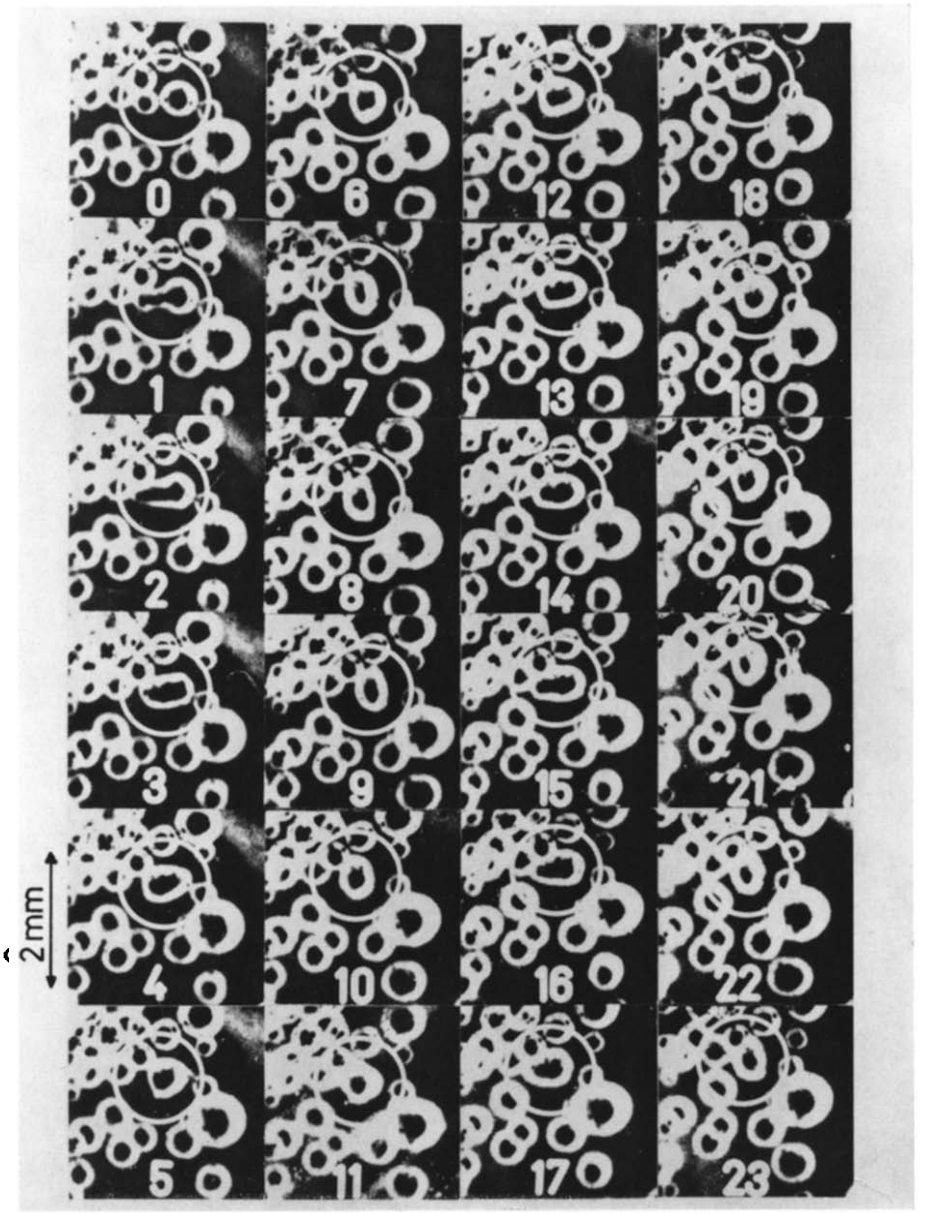

FIG. 4. 6·0 *wt. % 1-butanol in water*. Series of consecutive frames at a rate of 6000 frames per s. The tendency for coalescense and subsequent oscillation of neighbouring bubbles has been diminished due to the Marangoni-effect in positive mixtures. The occurrence of clusters of small bubbles is observed in these mixtures.

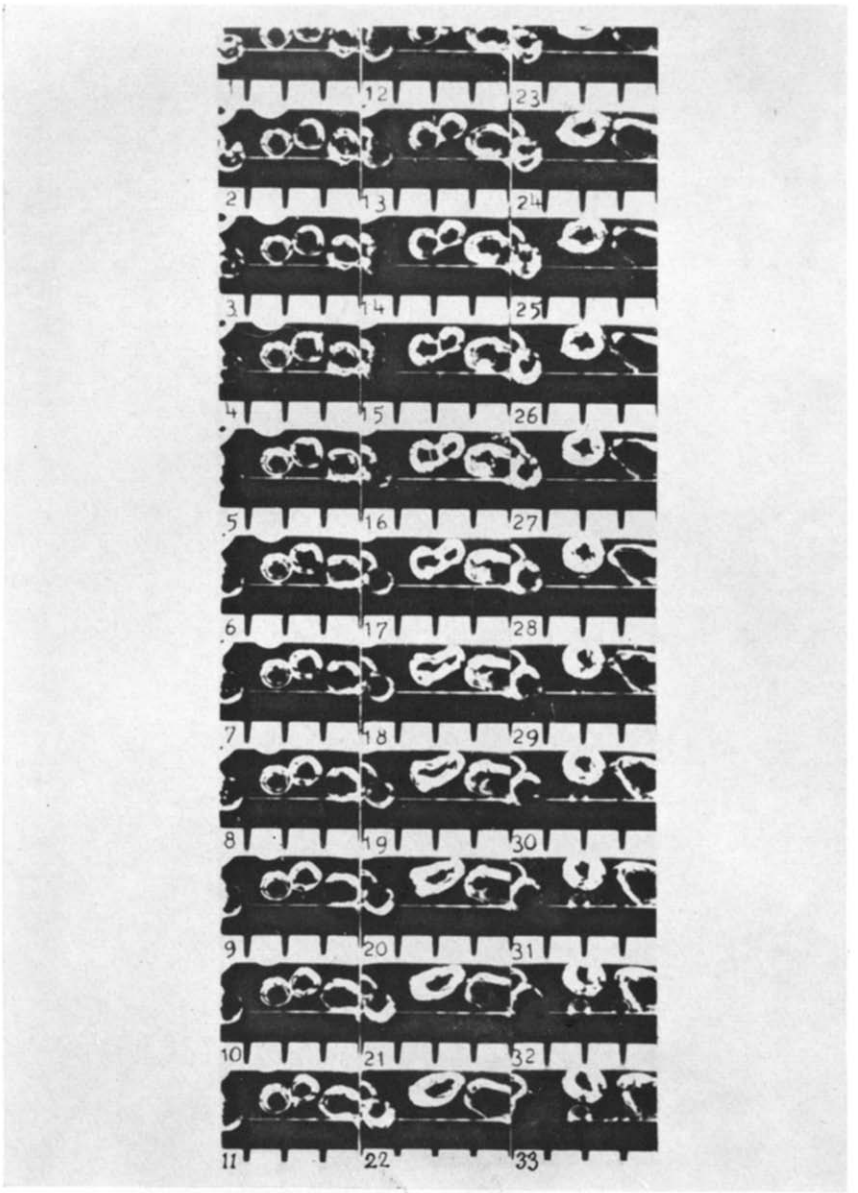

FIG. 5. *Water*. Nucleate boiling at atmospheric pressure. Series of consecutive frames at a rate of 5700 frames per s.

Two vapour bubbles, generated at neighbouring nuclei, coalesce after departure. The resulting bubble oscillates about the spherical shape.

The initial formation of the succeeding bubbles is shown in pictures 29 and 30, respectively, the rapid initial bubble growth in pictures 29–32. A 2-mm scale is visible at the bottom of the photographs.

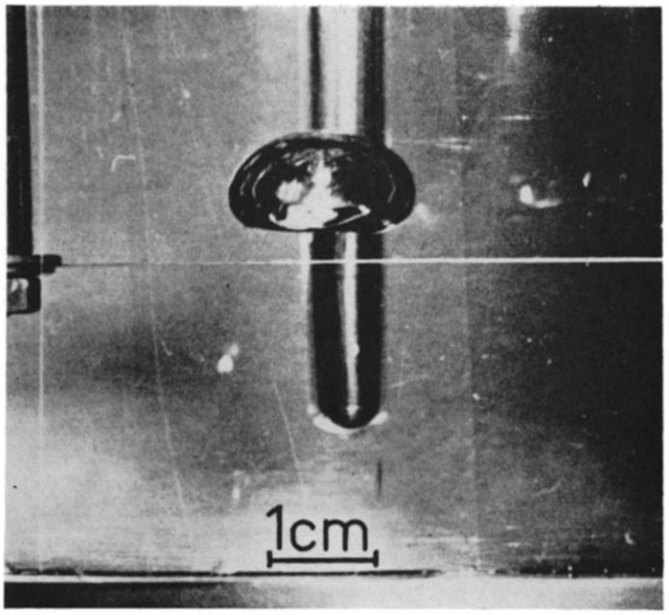

FIG. 10. *Water*. Intermittent occurrence of large vapour bubbles at a pressure of 0·13 ata.

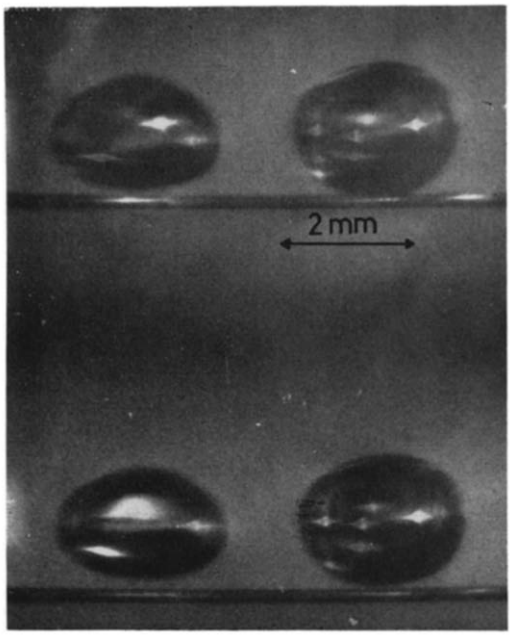

FIG. 11. *Water*. Succeeding pictures of vapour bubbles at atmospheric pressure, taken at a rate of 3000 frames per s.

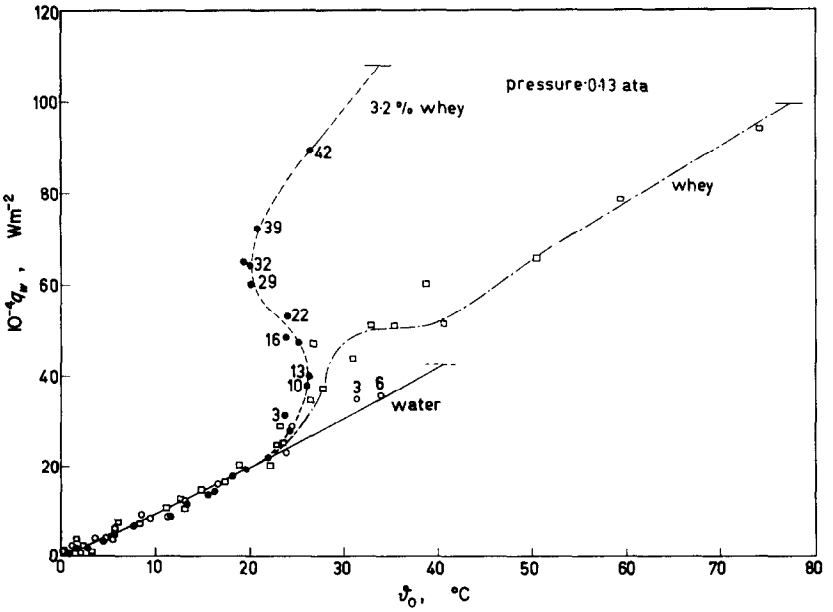

FIG. 7. Boiling curve for whey, for a dilution containing 3·2 vol. % whey in water, and for water, at a pressure of 0·13 ata.

The figures at the curves denote the number of active nuclei generating vapour bubbles on a square cm of the platinum heating wire.

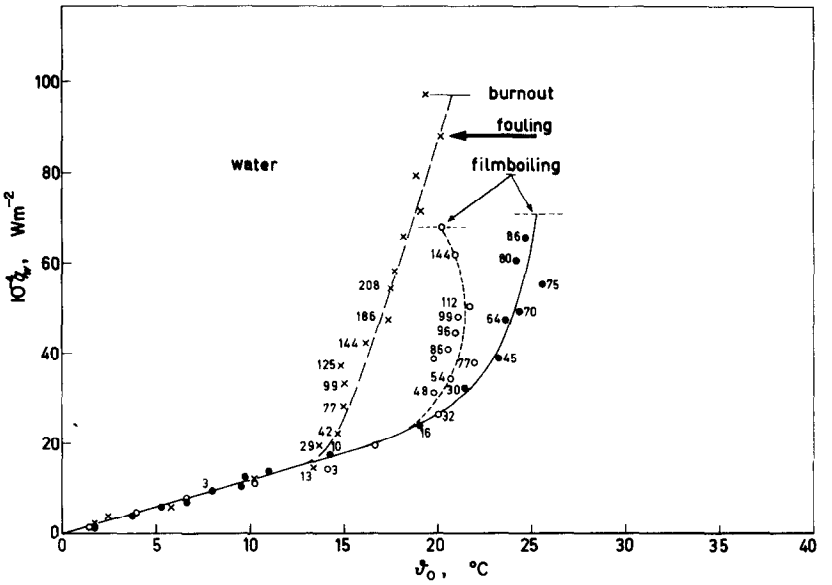

FIG. 8. *Water.* Effect of a gradual fouling (—— ——, — — — —) of the platinum heating wire, which originates from the pertinax cover of the boiling vessel in comparison to the boiling curve for a clean wire (————).

The fouling causes an increase in the coefficient of heat transfer, which is due to the action of a larger number of active nuclei generating smaller vapour bubbles. The figures at the curves denote the number of nuclei generating bubbles on a square cm of the wire.

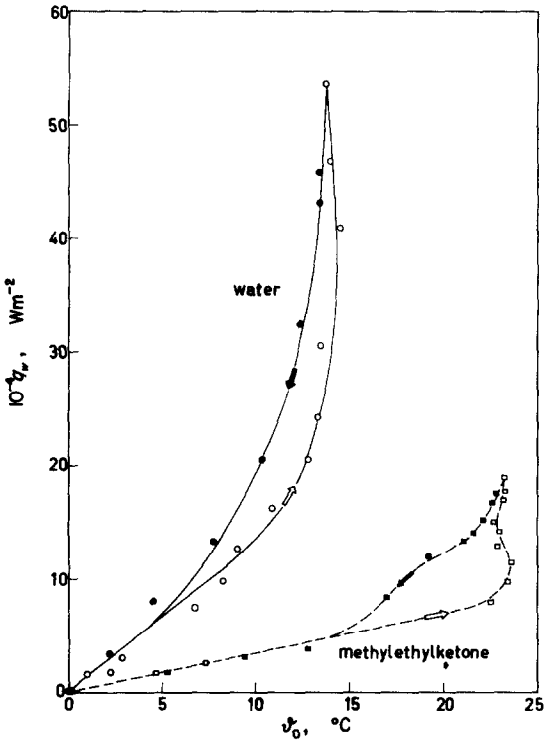

FIG. 9. *Methylethylketone.* Hysteresis effect in nucleate boiling due to a gradual contamination of the heating wire with free sulphur, which originates from an expanded Neoprene–rubber packing.

Water. Similar hysteresis effect. The increased coefficient of heat transfer for the descending branch of the curves is caused by a larger density of active nuclei, cf. Fig. 8.

increasing pressure, due to $C_1 \sim 1/\rho_2 \sim 1/p$. A large theoretical bubble radius R_1 (55×10^{-4} m) and a low frequency are predicted in water, boiling at a subatmospheric pressure of 0·13 ata, in quantitative agreement with the experimental value (compare Figs. 10 and 11).

Séméria [33] investigated the departure radius of independent bubbles on thin heating wires in water, boiling at pressures from 1 to 140 ata. The experimental results are: e.g. $\overline{R_1} = 8 \times 10^{-4}$ m at atmospheric pressure (cf. our value $9{\cdot}2 \times 10^4$ m, Section 4·3 of [3]), and $\overline{R_1} = 5 \times 10^{-6}$ m at 100 ata. These values shall be compared now with the theory: the product $bC_1\theta_{0,\max}$ in the expression (45) of [2] for R_1 decreases then to $1{\cdot}0 \times 10^{-3}$ m/s$^{\frac{1}{2}}$, and C_1 from 24×10^{-4} m/s$^{\frac{1}{2}}$ degC to 8×10^{-5} m/s$^{\frac{1}{2}}$ degC. Consequently, t_1 decreases from approximately $5{\cdot}0 \times 10^{-3}$ s to $1{\cdot}7 \times 10^{-4}$ s, whence $t_1^{\frac{1}{2}} = 1{\cdot}3 \times 10^{-2}$ s$^{\frac{1}{2}}$ at 100 ata, which yields $\overline{R_1} = 5 \times 10^{-6}$ m then; this agrees exactly with Séméria's value. The corresponding theoretical bubble frequency increases very rapidly to 1500 s^{-1}. Van Stralen [13] has shown, that $q_{w,\max}$ of water and aqueous binary mixtures is independent of the heating material at elevated pressures above 50 ata. Probably, this holds also for R_1. This effect is following from the expression for the equilibrium radius $R_0 = 2\sigma T/\rho_2 l\theta_0$, whence $R_0 \to 0$ at high pressures. Even the small roughnesses on smooth surfaces are suitable then for bubble generation.

REFERENCES

1. K. E. FORSTER and R. GREIF, Heat transfer to a boiling liquid-mechanism and correlations, *J. Heat Transfer* **81**, 43–53 (1959).
2. S. J. D. VAN STRALEN, The mechanism of nucleate boiling in pure liquids and in binary mixtures—Part I, *Int. J. Heat Mass Transfer* **9**, 995–1020 (1966).
3. S. J. D. VAN STRALEN, The mechanism of nucleate boiling in pure liquids and in binary mixtures—Part II, *Int. J. Heat Mass Transfer* **9**, 1021–1046 (1966).
4. F. C. GUNTHER and F. KREITH, Photographic study of bubble formation in heat transfer to subcooled water, Prog. Rep. No. 4–120, Jet Propulsion Lab., California Inst. of Technology (1950).
5. H. GRÖBER, S. ERK and U. GRIGULL, *Die Grundgesetze der Wärmeübertragung*, 3rd edn. Springer, Berlin, Göttingen, Heidelberg (1955).
6. F. D. MOORE and R. B. MESLER, The measurement of rapid surface temperature fluctuations during nucleate boiling of water, *A.I.Ch.E. Jl* **7**, 620–624 (1961).
7. N. MADSEN, Temperature fluctuations at a heated surface supporting pool boiling water, Lab. Rep., Laboratory of heat transfer and reactor engineering, Technological University of Eindhoven, The Netherlands (1964); Symposium on boiling heat transfer in steam-generated units and heat exchangers, Manchester, Paper No. 14 (1965), *Proc. Instn Mech. Engrs.* To be published.
8. T. F. ROGERS and R. B. MESLER, An experimental study of surface cooling by bubbles during nucleate boiling of water, *A.I.Ch.E. Jl* **10**, 656–660 (1964).
9. C. BONNET, E. MACKE and R. MORIN, Visualisation de l'ébullition nuclée de l'eau à pression atmosphérique et mesure simultanée des variations de température de surface, Centre commun de recherche nucléaire, Etablissement d'Ispra-Italy, Euratom Rep. Eur. 1622.f (1964).
10. S. J. D. VAN STRALEN, Heat transfer to boiling binary liquid mixtures at atmospheric and subatmospheric pressures, *Chem. Engng Sci.* **5**, 290–296 (1965).
11. R. SÉMÉRIA, An experimental study of the characteris-

tics of vapour bubbles, Symposium on two-phase fluid flow, Paper No. 7, Instn Mech. Engrs (1962).
12. E. MACKE, Private communication (1966).
13. S. J. D. VAN STRALEN, Warmteoverdracht aan kokende binaire vloeistofmengsels, Doctor thesis, Univ. of Groningen, The Netherlands; Veenman, Wageningen, The Netherlands (1959); *Meded. LandbHoogesch. Wageningen* **59**(6) (1959). In Dutch with English summary and captions.
14. M. JAKOB, *Heat Transfer*, Vol. 1. Wiley, New York; Chapman & Hall, London (1950).
15. S. J. D. VAN STRALEN, Het mechanisme van kernkoken, *Ned. Tijdschr. Natuurk.* **33**, 29–41, 65–87 (1967). In Dutch.
16. S. J. D. VAN STRALEN, De kookparadox in binaire vloeistofmengels, *Ingenieur, 's Grav.* To be published. In Dutch with English summary.
17. J. N. ADDOMS, Heat transfer at high rates to water boiling outside cylinders, Sc.D. thesis in chemical engineering, Massachusetts Inst. Technology (1948).
18. W. H. MCADAMS, *Heat Transmission*, 3rd edn. McGraw–Hill, New York (1945).
19. N. ZUBER, On the stability of boiling heat transfer, *Trans. Am. Soc. Mech. Engrs* **80**, 711–720 (1958).
20. N. ZUBER and M. TRIBUS, Further remarks on the stability of boiling heat transfer, Rep. 58-5, Dept. of Engng, Univ. of California, Los Angeles (1958).
21. E. A. KAZAKOVA, The maximum heat transfer to boiling water at high pressure, *Izv. Akad. Nauk SSSR. Otdel. Tekh. Nauk* (1), 1377–1387 (1950); *Eng. Dig., Los Angeles* **12**, 81–85 (1951).
22. M. T. CICHELLI and C. F. BONILLA, Heat transfer to liquids boiling under pressure, *A.I.Ch.E. Jl* **41**, 755–787 (1945).
23. F. J. G. KWANTEN, Private communication (1966); Kritieke verschijnselen bij de warmteoverdracht aan kokende unaire en binaire vloeistoffen, to be published in *Ingenieur, 's Grav.* **79** (1967). In Dutch with English summary.
24. J. HOVESTREIJDT, The influence of the surface tension difference on the boiling of mixtures, *Chem. Engng Sci.* **18**, 631–639 (1963).
25. R. W. VAN HOESEN KORNDORFFER, Warmteoverdracht aan kokende binaire mengsels van organische stoffen, Rep. No. N 60/29, Rep. No. P 60/18, Centraal Lab. T.N.O., Delft (1960). In Dutch.
26. S. J. D. VAN STRALEN, Transition from nucleate boiling to filmboiling in ethanol (High-speed motion picture), Agric. Univ., Wageningen (1960).
27. S. J. D. VAN STRALEN, Heat transfer to boiling skim-milk, *Netherl. J. Agric. Sci.* **4**, 107–110 (1956); *Meded. LandbHoogesch. Wageningen* **56**(3), 1–11 (1956).
28. S. J. D. VAN STRALEN, Heat transfer to boiling binary liquid mixtures, *Br. Chem. Engng* **4**, 8–17 (1959); **4**, 78–82 (1959); **6**, 834–840 (1961); **7**, 90–97 (1962).
29. E. A. FARBER and R. L. SCORAH, Heat transfer to water boiling under pressure, *Trans. Am. Soc. Mech. Engrs* **70**, 369–384 (1948).
30. P. OGDEN and R. L. SCORAH, The effect of high temperature steam on a nickel–chromium–iron alloy, *Bull. Univ. MO. Engng. Ser.* 38, **53**(16) (1952).
31. H. HAMPSON, J. S. TURTON and L. A. SUTHERLAND, The effects of solid additives on the saturated pool-boiling of water, Symposium on boiling heat transfer in steam-generated units and heat exchangers, Manchester, Paper No. 8 (1965), *Proc. Instn Mech. Engrs.* To be published.
32. J. W. PALEN and J. W. WESTWATER, Heat transfer and fouling rates during poolboiling of calcium sulfate solutions, *Chem. Engng Prog. Symp. Ser.* **62**, 77–86 (1966).
33. R. SÉMÉRIA, An experimental study of the characteristics of vapour bubbles, Symposium on two-phase fluid flow, Paper No. 7. Instn Mech. Engrs (1962).

APPENDIX

Numerical Values

1. *Water*

One evaluates $\alpha\ h_{w,co} = 7730\ \theta_0^{\frac{1}{3}}$ from the boiling curve for water from Fig. 1 of [2], whence equation (13) yields a $t_{1,\max}^{\frac{1}{2}} = 4{\cdot}09 \times 10^{-2}\ s^{\frac{1}{2}}$ at $\theta_{0,\max} = 21{\cdot}5$ degC. This is resulting —according to equations (5) and (14)—in a $q_{w,\max} = (33 + 49) \times 10^4\ W/m^2 = 82 \times 10^4\ W/m^2$, i.e. an increase of approximately 30 per cent in comparison to the theoretical value predicted by equation (73) of [3]. The average experimental value amounts to $67 \times 10^4\ W/m^2$, cf. Table 3 of [3].

The lower peak flux ($59 \times 10^4\ W/m^2$ in Fig. 1 obtained with d.c. heating) is corresponding to a lower $h_{w,co} = 4850\ \theta_0^{\frac{1}{3}}$, an increased $t_{1,\max}^{\frac{1}{2}} = 5{\cdot}87 \times 10^{-2}\ s^{\frac{1}{2}}$ and an increased wire superheating necessary to activate the first nucleus for bubble formation, which is resulting in a higher $\theta_{0,\max} = 31{\cdot}5$ degC.

The deviation is due to the use of boiling vessels of a different construction. In the latter case, the contribution of the forced convection caused by the liquid flow ascending from the heated bottom plate, is lowered due to the attachment of a "bubble screen". This sheet keeps vapour bubbles moving upwards from the front side of the boiling vessel out of vision in case of photographic recordings.

2. 4·1 % *methylethylketone*

The theoretical peak flux in this mixture amounts to $q_{w,\max} = (51 + 163) \times 10^4\ W/m^2 =$

214×10^4 W/m^2 (experimental value: 172×10^4 W/m^2) according to equation (10), as $t^{\ddagger}_{1,\max} = 3{\cdot}61 \times 10^{-2}$ s‡ at $\theta_{0,\max} = 34$ degC. The ratio of the theoretical peak flux in this mixture to the value in water (2·6) is in quantitative agreement with the experimental data, cf. Fig. 1 of [2].

In contradistinction to the behaviour of water (Fig. 1), new measurements for 4·1% methylethylketone yielded the following results in the lower part of the region of nucleate boiling: $q_w = 48{\cdot}5 \times 10^4$ W/m^2 at $\theta_0 = 35{\cdot}0$ degC, $q_{w,co} = 25{\cdot}2 \times 10^4$ W/m^2, whence $q_{w,bi} = q_{w,b}/q_{w,bi} = 0{\cdot}17$. For a higher heat flux $q_w =$ the direct vapour formation at the heating surface amounts to $q_{w,b} = 4{\cdot}03 \times 10^4$ W/m^2, i.e. $q_{w,b}/q_{w,bi} = 0{\cdot}17$. For higher heat flux $q_w = 84{\cdot}0 \times 10^4$ W/m^2 at $\theta_0 = 35{\cdot}4$ degC, $q_{w,co} = 25{\cdot}8 \times 10^4$ W/m^2, whence $q_{w,bi} = 58{\cdot}2 \times 10^4$ W/m^2; the corresponding $q_{w,b} = 5{\cdot}4 \times 10^4$ W/m^2, i.e. $q_{w,b}/q_{w,bi} = 0{\cdot}09$, cf. the estimated value (0·10) in Table 1 of [3].

The experimental value of the ratio is decreasing for increasing heat flux and is smaller than the theoretical (0·40) predicted by equation (11). This is due to the presence of a gradually increasing numbers of very small bubbles "complex nuclei", cf. [2] and [3], with a diminishing $C_{1,m}$, which finds particularly expression in the right-hand side of equation (3) on account of the growth constant, which is missing in equation (2).

3. *Effect of θ_0 on R_1 and ν in water*

It may be noticed, that equation (45) of [2] predicts a linear increase of R_1 with θ_0:

$$R_1 = (b/\mathrm{e})\, C_1 \theta_0\, u_1, \tag{29}$$

whence $\nu R_1^2 = \{(b/2\mathrm{e})C_1\theta_0\}^2$ should be independent of t_1. For a large number of bubbles in water, the experimental R_1 was nearly independent of the value of θ_0 in nucleate boiling. However, the bubble frequency ν on a nucleus increased gradually with increasing θ_0. This behaviour can be understood by considering the fact that a nucleus, once being activated at θ_0, needs no higher superheating to generate bubbles, even not at the peak flux; i.e. in this case the local liquid nearby the nucleus is superheated then periodically up to θ_0, and not to $\theta_{0,\max}$. Hence, R_1 may be expected to be independent of θ_0—cf. also equation (13)—but the waiting time t_2 is shortened. This corresponds to an increased bubble frequency.

The behaviour of some succeeding bubbles generated on the same spot has been studied by using the motion pictures, which were taken with a high speed framing camera for Fig. 1. The nearly constant speed of the last 8 m of the film amounted to 5750 frames per s. The concerning spot on the heating wire generated relatively large bubbles. This was due to a coalescence of two neighbouring bubbles, which originated from separate nuclei. These nuclei were active only for $\theta_0 > 23$ degC. At $\theta_0 = 26{\cdot}5$ degC the following frame numbers are of importance: Bubble 1: originates at nr. 0, t_1 at nr. 51, $R_1 = 9{\cdot}2 \times 10^{-4}$ m. Bubble 2: originates at nr. 93, t_1 at nr. 173, $R_1 = 11{\cdot}5 \times 10^{-4}$ m. Bubble 3: originates at nr. 303, t_1 at nr. 355, $R_1 = 9{\cdot}0 \times 10^{-4}$ m. Bubble 4: originates at nr. 404, t_1 at nr. 474, $R_1 = 11{\cdot}3 \times 10^{-4}$ m. At $\theta_0 = 29{\cdot}85$ degC: Bubble I: originates at nr. 0, t_1 at nr. 49, $R_1 = 10{\cdot}8 \times 10^{-4}$ m. Bubble II: originates at nr. 83, t_1 at nr. 126, $R_1 = 10{\cdot}4 \times 10^{-4}$. Bubble III: originates at nr. 153, t_1 at nr. 220, $R_1 = 12{\cdot}7 \times 10^{-4}$ m. Bubble IV: originates at nr. 240, t_1 at nr. 301, $R_1 = 12{\cdot}0 \times 10^{-4}$ m.

Hence, at $\theta_0 = 26{\cdot}5$ degC: $\overline{R_1} = 10{\cdot}25 \times 10^{-4}$ m, $\bar{t}_1 = 63{\cdot}2$ frames, $\bar{t}_2 = 73{\cdot}7$ frames, $t_2/t_1 = 1{\cdot}16$ (theoretical value for separate bubbles: 3·00), $\bar{\nu} = 50$ s^{-1}, $b = 0{\cdot}45$ follows from (29), $\bar{\nu}\overline{R_1^2} = 5{\cdot}3 \times 10^{-5}$ m^2/s (theoretical value for separate bubbles with $b = 0{\cdot}70$—cf. the Appendix of [3]—$6{\cdot}7 \times 10^{-5}$ m^2/s). At $\theta_0 = 29{\cdot}85$ degC: $\overline{R_1} = 11{\cdot}47\,10^{-4}$ m, $\bar{t}_1 = 55{\cdot}0$ frames, $\bar{t}_2 = 27{\cdot}0$ frames, $t_2/t_1 = 0{\cdot}50$, $\bar{\nu} = 85$ s^{-1}, $b = 0{\cdot}48$ follows from (29), $\bar{\nu}\overline{R_1^2} = 11{\cdot}2 \times 10^{-5}$ m^2/s (theoretical value for $b = 0{\cdot}70$: $8{\cdot}5 \times 10^{-5}$ m^2/s).

The increase of both $\overline{R_1}$ and θ_0 amounts to 12 per cent, whence $\overline{R_1}$ is proportional to θ_0

here. The increase in v, however, is much larger, viz. 70 per cent. The contribution of the nucleus in $q_{w,b}$ has thus been increased in the ratio $(1{\cdot}12)^3$ $1{\cdot}70 = 2{\cdot}39$. The low value of t_2/t_1 at a constant θ_0 is due to the premature bubble coalescence at the heating wire, as t_1 has been increased in comparison to separate bubbles and t_2 has been decreased with the same amount. The low value of the growth parameter b can be attributed to the same reason: the regions of influence of neighbouring bubbles may overlap, whence the full radius predicted from two independent separate bubbles is not reached in case of interaction.

The study of twenty-eight bubbles at $\theta_0 = 26{\cdot}5$ degC on 4·37 active spots (some spots are active only off and on) yielded: $\bar{R}_1 \times 13{\cdot}7 \times 10^{-4}$ m, $t_2/t_1 = 4{\cdot}21$ assuming $b = 0{\cdot}70$, $\bar{\nu} = 27$ s^{-1} and $\bar{\nu}\bar{R}_1^2 = 5{\cdot}1 \times 10^{-5}$ m^2/s. Eighty partly coalescing bubbles (corresponding with 130 separate bubbles) at $\theta_0 = 29{\cdot}85$ degC on 9·25 active spots (corresponding with seventeen nuclei) were giving: $\bar{R}_1 = 13{\cdot}2 \times 10^{-4}$ m ($\bar{R}_1 = 11{\cdot}2 \times 10^{-4}$ m for separate bubbles), $t_2/t_1 = 3{\cdot}36$, assuming $b = 0{\cdot}70$, $\bar{\nu} = 45\ s^{-1}$ ($\bar{\nu} = 40\ s^{-1}$ for separate bubbles) and $\bar{\nu}\bar{R}_1^2 = 7{\cdot}8 \times 10^{-5}$ m^2/s. The increase of $\bar{\nu}$ with increasing θ_0 is evident, the independence of $\bar{R}_1$ of θ_0 also, for a large number of bubbles investigated.

CORRIGENDA

Corrections in Part I [2] *and Part II* [3]

Part I: p. 1015, caption of Fig. 7: "l_1" should be read "t_1"; p. 1015, equation (50): "$\left(2\ 1 - \frac{2}{e}\right)$" should read "$2\left(1 - \frac{2}{e}\right)$".

Part II: p. 1033, caption of Fig. 2: "Δ/G_d" should be read "$\Delta T/G_d$"; p. 1039, the denominator in the right-hand side of the equation in Section 4.4. "$\frac{1}{4}t_{1,p}$" should be read "$1/(4t_{1,p})$"; footnote † to Table 1: "on some nucleus" should be read "on same nucleus".

Part I: p. 1005. According to a private communication by Professor Madsen, his interpretation of large temperature dips observed during film boiling is based on partial liquid contact (at moderate superheatings), which has recently been established by W. S. Bradfield, *I/EC Fundamentals* **5**, 200–204 (1966).

Résumé—On a corrigé la théorie de l'auteur sur la "microcouche de relaxation" pour le mécanisme de l'ébullition nucléée en réservoir afin de tenir compte du maximum élevé du flux qui se produit à une faible concentration du constituant le plus volatil dans les mélanges liquides binaires, cf. Parties I et II. Le soutirage de chaleur à partir de la surface chauffante se produit pendant la plus grande partie du temps de contact et pendant toute la période de retard suivante, (c'est-à-dire, presque continuellement), et peut être décrite par la conduction pure seulement. En conséquence, on montre que l'hypothèse de Gunther et Kreith de la "microconvection dans la sous-couche normalement laminaire" n'est pas nécessaire. On a obtenu une expression pour le flux maximal en fonction de la contribution correspondante de la convection. Dans les liquides purs, on montre que la production directe de vapeur à la paroi est responsable de toute l'augmentation de flux de chaleur au-dessus de celui dû à la convection pour une surchauffe arbitraire dans le région de l'ébullition nucléée, en accord quantitatif avec les données expérimentales, grâce à des films pris à grande vitesse dans le cas de l'eau.

Le rayon de départ des bulles et le flux maximal sont étudiés en fonction de la pression. La taille des bulles diminue rapidement lorsque la pression augmente, en accord quantitatif avec les résultats obtenus par Séméria sur de l'eau à pression élevée et par l'auteur également sur de l'eau mais à des pressions au-dessous de la pression atmosphérique. La surchauffe critique dans l'ébullition nucléée diminue lorsque la pression augmente, en accord avec les résultats d'Addom.

L'effet favorable d'un léger degré de saleté de la surface de chauffage sur les propriétés de nucléation et en conséquence sur le coefficient correspondant de transport de chaleur, qui avait été découvert auparavant par l'auteur, est discuté en le comparant avec des résultats supplémentaires récents d'autres auteurs.

Finalement, l'existence d'un effet d'hystérésis dans l'ébullition est due à la saleté de la surface.

Zusammenfassung—An der "relaxation microlayer" Theorie des Autors für Blasensieden wurden Korrekturen angebracht, die dem grossen maximalen Wärmefluss Rechnung tragen, der bei geringer Konzentration der leichter flüchtigen Komponente eines binären Gemisches auftritt. (s. Teil I–II).

Die Wärmeabfuhr von der Heizfläche erfolgt während des grössten Teils der Zeit des Blasenwachstums und während der ganzen Wartezeit (d.h. fast kontinuierlich) und kann nur durch reine Leitung beschrieben werden. Folglich, so wird gezeigt, ist die Hypothese von Gunther and Kreith, über eine Mikrokonvektion in der Grenzschicht, überflüssig. Ein Ausdruck für den maximalen Wärmestrom in Abhängigkeit von der entsprechenden konvektiven Verteilung wurde hergeleitet. Es wird gezeigt, dass im Bereich des Blasensiedens von reinen Flüssigkeiten bei willkürlicher Überhitzung das gesamte Anwachsen des Wärmestroms gegenüber der freien Konvektion auf die unmittelbare Dampferzeugung an der Wand zurückzuführen ist. Darin besteht quantitative Übereinstimmung mit Versuchsergebnissen, die aus Hochgeschwindigkeitsaufnahmen an Wasser gewonnen wurden.

Sowohl der Blasenabreissradius, als auch der maximale Wärmefluss, werden in Abhängigkeit vom Druck untersucht. Die Blasengrösse nimmt bei wachsendem Druck sehr stark ab, in quantitativer Übereinstimmung mit Versuchen an Wasser von Séméria bei erhöhtem, und mit Versuchen vom Autor, bei vermindertem Luftdruck. In Übereinstimmung mit Addom wird gezeigt, dass sich die kritische Überhitzung beim Blasensieden mit zunehmendem Druck vermindert.

Der früher vom Autor entdeckte günstige Einfluss geringer Verunreinigungen der Heizfläche auf die Keimbildung und somit auf die Wärmeübergangskoeffizienten, wird im Vergleich mit neueren Arbeiten anderer Forscher diskutiert. Schliesslich wird gezeigt, dass der Hyster siseffekt beim Sieden eine Folge von Verunreinigungen ist.

Аннотация—Теория «релаксации микрослоя», предложенная автором для механизма пузырькового кипения в большом объеме, распространяется для учета больших пиков тепловых потоков при низкой концентрации более летучего компонента в бинарных жидких смесях (см. ч. 1–2). Теплосъем с поверхности нагрева происходит почти во вси время прилипания и занимает большую часть периода задержки (т.е. происходит почти постоянно) и может быть описан чистой теплопроводностью. Следовательно, гипотеза «микроконвекции в нормальном ламинарном подслое» Гунтера и Крейтса не является необходимой. Выведено выражение для максимального теплового потока в зависимости от соответствующей величины конвективной составляющей. Показано, что в чистых жидкостях образование пара на стенке является причной всего превышения теплового потока над конвективным при произвольном перегреве в области пузырькового кипения, что находится в количественном соответствии с экспериментальными данными для воды, полученными с помощью высокоскоростной киносъемки. Радиус отрыва пузырька и максимальный тепловой поток исследуются в зависимости от давления. Размеры пузырька быстро уменьшаются при увеличении давления, что находится в количественном соответствии с данными Семериа при повышенном давлении и результатами автора при давлении ниже атмосферного. Показано, что критический перегрев при пузырьковом кипении уменьшается при увеличении давления, что находится в соответствии с данными Адамса. Благоприятное влияние не очень сильного образования накипи на поверхности нагрева на её свойства с точки зрения наличия центров парообразования, обнаруженное ранее автором, обсуждается в сравнении с более поздними результатами других исследователей. Наконец, показано, что эффект гистерезиса возникает в результате образования накипи.